

Interactions between Titanium Dioxide and Phosphatidyl Serine-Containing Liposomes: Formation and Patterning of Supported Phospholipid Bilayers on the Surface of a Medically Relevant Material

Fernanda F. Rossetti,[†] Marta Bally,[†] Roger Michel,^{†,§} Marcus Textor,^{*,†} and Ilya Reviakine^{*,‡}

BioInterfaceGroup, Laboratory for Surface Science and Technology, Department of Materials, Swiss Federal Institute of Technology (ETH), CH-8093 Zürich, Switzerland, and Department of Physical Chemistry, Technical University Clausthal, D-38678 Clausthal-Zellerfeld, Germany

Received April 6, 2005

Titanium is widely used in biomedical applications. Its mechanical properties and biocompatibility, conferred by a layer of oxide present on its surface, make titanium the material of choice for various implants (artificial hip and knee joints, dental prosthetics, vascular stents, heart valves). Furthermore, the high refractive index of titanium oxide is advantageous in biosensor applications based on optical detection methods. In both of the above fields of application, novel surface modification strategies leading to biointeractive interfaces (that trigger specific responses in biological systems) are continuously sought. In this report, we investigate the interactions between TiO₂ and phosphatidyl serine-containing liposomes, present a novel approach for preparing supported phospholipid bilayers (SPBs) of various compositions on TiO₂, and use the unique ability of liposomes to distinguish between different surfaces to create SPB corrals on SiO₂/TiO₂ structured substrates. These results represent an important first step toward the design of biointeractive interfaces on titanium oxide surfaces that are based on a cell membrane-like environment.

Introduction

In recent years, the focus of biocompatibility-related research has shifted from the reduction of negative responses caused by implanted materials in biological hosts to designing interactive biointerfaces capable of evoking specific effects in biological systems (e.g., wound healing, cell differentiation, etc.^{1–3}). In this context, there is a growing interest in exploring the properties of surfaces coated with supported phospholipid bilayers (SPBs^{4–6}),⁷ due to their cell membrane-like structure, biocompatibility, and ease with which various functionalities can be incorporated into them (e.g., receptors for eukaryotic cell attachment,⁸ antibody fragments,⁹ receptors for bacterial toxins,¹⁰ G-protein coupled receptors,¹¹ and nucleic acids^{12–14}). Various approaches to patterning SPBs have also been reported.^{11,15–23}

Titanium is a widely used implant material (Figure 1a). It is found in artificial hip and knee joints, dental prosthetics, ventricular assist devices, heart valves, and vascular stents.²⁴ The success of titanium in implant technology is to a large extent due to its biocompatibility, conferred by a native layer of oxide that coats the metal's surface.²⁵ Furthermore, the high refractive index of the oxide makes it an attractive material for use in biosensor technology (Figure 1a).²⁶

In this Article, we report the formation of supported bilayers on titanium oxide surfaces, bringing the unique advantages of the supported bilayer methodology to the surface of a medically relevant material—a development that is expected to open new venues in biomaterial and biosensor research (Figure 1). While SPBs are routinely prepared from liposomes on silica, glass, and mica, this is not the case with TiO₂, to which zwitterionic liposomes

* Corresponding author. Telephone: +49 (0)532 372 37 89. Fax: +49 (0)532 372 48 35. E-mail: ireviakine@uh.edu.

[†] Swiss Federal Institute of Technology.

[‡] Technical University Clausthal.

[§] Current address: Department of Chemical Engineering, University of Washington, Seattle, WA 98195-1750.

(1) Tirrell, M.; Kokkoli, E.; Biesalski, M. *Surf. Sci.* **2002**, *500*, 61–83.
 (2) Puleo, D. A.; Nanci, A. *Biomaterials* **1999**, *20*, 2311–2321.
 (3) Shin, H.; Jo, S.; Mikos, A. G. *Biomaterials* **2003**, *24*, 4353–4364.
 (4) Tamm, L. K.; McConnell, H. M. *Biophys. J.* **1985**, *47*, 105–113.
 (5) McConnell, H. M.; Watts, T. H.; Weis, R. M.; Brian, A. A. *Biochim. Biophys. Acta* **1986**, *864*, 95–106.
 (6) Sackmann, E. *Science* **1996**, *271*, 43–48.
 (7) Kasemo, B. *Surf. Sci.* **2002**, *500*, 656–677.
 (8) Svedhem, S.; Dahlborg, D.; Ekeröth, J.; Kelly, J.; Höök, F.; Gold, J. *Langmuir* **2003**, *19*, 6730–6736.
 (9) Vikholm, I.; Viitala, T.; Albers, W. M.; Peltonen, J. *Biochim. Biophys. Acta* **1999**, *1421*, 39–52.
 (10) Mou, J. X.; Yang, J.; Shao, Z. F. *J. Mol. Biol.* **1995**, *248*, 507–512.
 (11) Heyse, S.; Ernst, O. P.; Dienes, Z.; Hofmann, K. P.; Vogel, H. *Biochemistry* **1998**, *37*, 507–522.
 (12) Yoshina-Ishii, C.; Boxer, S. G. *J. Am. Chem. Soc.* **2003**, *125*, 3696–3697.

(13) Olson, D. J.; Johnson, J. M.; Patel, P. D.; Shaqfeh, E. S. G.; Boxer, S. G.; Fuller, G. G. *Langmuir* **2001**, *17*, 7396–7401.

(14) Larsson, C.; Rodahl, M.; Höök, F. *Anal. Chem.* **2003**, *75*, 5080–5087.

(15) Lenz, P.; Ajo-Franklin, C. M.; Boxer, S. G. *Langmuir* **2004**, *20*, 11092–11099.

(16) Hovis, J. S.; Boxer, S. G. *Langmuir* **2001**, *17*, 3400–3405.

(17) Boxer, S. G. *Curr. Opin. Chem. Biol.* **2000**, *4*, 704–709.

(18) Hovis, J. S.; Boxer, S. G. *Langmuir* **2000**, *16*, 894–897.

(19) Groves, J. T.; Ulman, N.; Cremer, P. S.; Boxer, S. G. *Langmuir* **1998**, *14*, 3347–3350.

(20) Ulman, N.; Groves, J. T.; Boxer, S. G. *Biophys. J.* **1997**, *72*, MP444–MP444.

(21) Svedhem, S.; Pfeiffer, I.; Larsson, C.; Wingren, C.; Borrebaeck, C.; Höök, F. *ChemBioChem* **2003**, *4*, 339–343.

(22) Yee, C. K.; Amweg, M. L.; Parikh, A. N. *J. Am. Chem. Soc.* **2004**, *126*, 13962–13972.

(23) Kam, L.; Boxer, S. G. *J. Am. Chem. Soc.* **2000**, *122*, 12901–12902.

(24) Brunette, D. M.; Tengvall, P.; Textor, M.; Thomsen, P., Eds. *Titanium in Medicine*; Springer-Verlag: Berlin, 2001.

(25) Kasemo, B. *J. Prosthet. Dent.* **1983**, *49*, 832–837.

(26) Kurat, R.; Textor, M.; Ramsden, J. J.; Böni, P.; Spencer, N. D. *Rev. Sci. Instrum.* **1997**, *68*, 2172–2176.

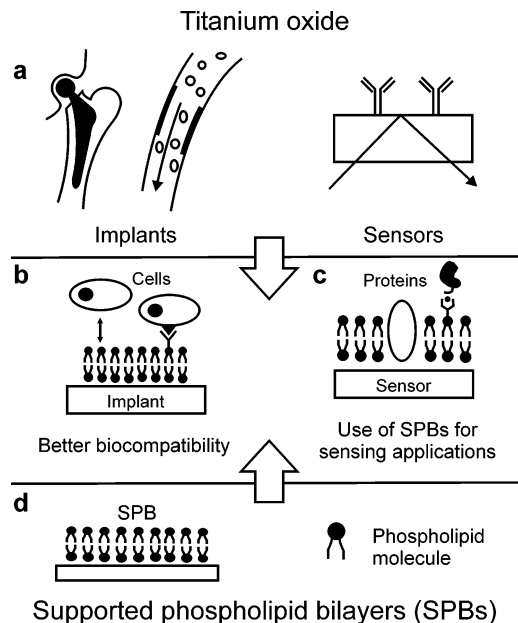


Figure 1. Titanium as a biomaterial and its combination with supported phospholipid bilayers (SPBs). (a) Examples of application of titanium oxide in implant and sensor technologies (from left to right): hip joint implants, vascular stents that dilate constricted blood vessels, biosensors based on an optical sensing technique. (b) Implants (for example, a vascular stent) coated with lipidic bilayers mimic cell membranes, resulting in a better biocompatibility and the possibility of targeting certain types of cells in the body by incorporating specific receptors in the bilayer. (c) The possibility of forming phospholipid bilayers on TiO_2 -based biosensors opens new venues in the biosensor research. For example, optical waveguide lightmode spectroscopy²⁶ that has not been compatible with SPB technology due to surface limitations can now be applied. (d) Structure of a supported phospholipid bilayer and of its constituting molecules. A phospholipid consists of a hydrophilic head (phosphatidylcholine or phosphatidylserine in this study) and two hydrophobic alkyl chains (oleoyl in this study). In aqueous solutions, lipids self-assemble into a variety of phases, of which the lamellar phase is one example.

adsorb intact^{27,28} (bilayer formation on TiO_2 reported previously by Starr et al.²⁹ may actually be due to silica contamination on the surface³⁰). The selectivity of biological systems with respect to various materials³¹ is far from being understood even in the case of relatively simple systems such as liposomes. Despite the large number of publications that have recently focused on the interactions of liposomes with various surfaces,^{27,28,32–39} understanding of these interactions remains elusive. A significant portion of this report is therefore dedicated to the details of

TiO_2 -liposome interactions. Their knowledge, in turn, allowed us to take advantage of the unique ability of liposomes to distinguish between different materials to prepare patterns of SPBs on prepatterned metal oxide substrates described previously.^{40,41}

Materials and Methods

Materials. The phospholipids used in this study, dioleoyl phosphatidyl choline (DOPC), dioleoyl phosphatidyl serine (DOPS), 1,2-dioleoyl-sn-glycero-3-[(N(5-amino-1-carboxypentyl)iminodiacetic acid) succinyl] (nickel salt) (DOGS-NTA-Ni), and fluorescently labeled nitrobenzoxadiazole-phosphatidyl choline (NBD-PC, excitation wavelength 488 nm), were purchased from Avanti Polar Lipids Inc. (Alabaster, AL). Biotinylated dioleoyl phosphatidyl ethanolamine (biotin-X-DOPE) and fluorescently labeled tetramethylrhodaminethylcarbamoyl phosphatidyl ethanolamine (TRITC-PE, excitation wavelength 543 nm) were obtained from Molecular Probes (Leiden, The Netherlands). Streptavidin was purchased from Fluka (Buchs, Switzerland). Green fluorescent protein (GFP) was kindly supplied by Eva Künemann (Institute for Molecular Biology and Biophysics, ETH Zürich, Switzerland).

Two different buffers were used throughout this study: Ca^{2+} buffer, containing 10 mM HEPES, 100 mM NaCl, and 2 mM CaCl_2 ; and EDTA buffer, containing 10 mM HEPES, 100 mM NaCl, 2 mM EDTA. In both cases, the pH was adjusted to 7.4 with NaOH. EDTA is a chelator of divalent cations such as Ca^{2+} . Chemicals were purchased from Sigma or Fluka (Buchs, Switzerland).

Vesicle Preparation. Unilamellar vesicles containing between 0% and 50% DOPS in DOPC (by weight) were prepared by extrusion with a Lipofast extruder (Avestin Inc., Ottawa, Canada) following established protocols (e.g., see refs 39, 42, 43).

Substrate Preparation and Cleaning. Gold-coated quartz crystals for use in the QCM-D experiments were purchased from Q-Sense AB (Gothenburg, Sweden) and coated with 12 nm of TiO_2 by reactive sputtering in a Leybold dc-magnetron Z600 sputtering unit at the Paul Scherrer Institut (Villigen, Switzerland) as described previously.²⁶ Round glass coverslips (Menzel Gläser, Braunschweig, Germany) coated with TiO_2 through the same procedure were used for fluorescence microscopy. Both kinds of substrates were cleaned in a 2% SDS solution for at least 30 min, rinsed with ultrapure water, and treated in a preheated UV/ozone cleaner (model 135500, Boekel Industries Inc., Feasterville, PA) for 30 min.

The $\text{SiO}_2/\text{TiO}_2$ patterned substrates were prepared as described in Lussi et al.⁴⁰ and cleaned by first sonicating them 15 min in a series of solvents (toluene, hexane, acetone, 2-propanol, ethanol, and water) and then treating them with oxygen plasma for 2 min immediately before the first use. For the subsequent uses, the patterned samples were cleaned with the same procedure as for nonpatterned surfaces (soaking in SDS solution followed by UV/ozone treatment; see above).

Quartz Crystal Microbalance with Dissipation (QCM-D).⁴⁴ QCM-D measurements were performed with a QE301 (electronics unit)/QAFC301 (axial flow chamber) instrument from Q-Sense AB (Gothenburg, Sweden) as described elsewhere.^{42,44} Briefly, a clean crystal was mounted in the flow chamber, which was then filled with the appropriate buffer. After the acquisition of a baseline, 0.5 mL of a temperature-equilibrated suspension of unilamellar vesicles at 0.5 mg/mL lipid concentration was injected into the measurement chamber. Frequency and dissipation signals were monitored until they stabilized. Excess of vesicles was removed by rinsing the measurement chamber with

(27) Reimhult, E.; Höök, F.; Kasemo, B. *Langmuir* **2003**, *19*, 1681–1691.

(28) Reviakine, I.; Rossetti, F. F.; Morozov, A. N.; Textor, M. *J. Chem. Phys.* **2005**, *122*, in press.

(29) Starr, T. E.; Thompson, N. L. *Langmuir* **2000**, *16*, 10301–10308.

(30) Ajo-Franklin, C. M.; Kam, L.; Boxer, S. G. *Proc. Natl. Acad. Sci. U.S.A.* **2001**, *98*, 13643–13648.

(31) Parsegian, V. A. *J. Prosthet. Dent.* **1983**, *49*, 838–842.

(32) Nollert, P.; Kiefer, H.; Jähnig, F. *Biophys. J.* **1995**, *69*, 1447–1455.

(33) Keller, C. A.; Kasemo, B. *Biophys. J.* **1998**, *75*, 1397–1402.

(34) Johnson, J. M.; Ha, T.; Chu, S.; Boxer, S. G. *Biophys. J.* **2002**, *83*, 3371–3379.

(35) Schönherr, H.; Johnson, J. M.; Lenz, P.; Frank, C. W.; Boxer, S. G. *Langmuir* **2004**, *20*, 11600–11606.

(36) Zhdanov, V. P.; Kasemo, B. *Langmuir* **2001**, *17*, 3518–3521.

(37) Richter, R.; Mukhopadhyay, A.; Brisson, A. *Biophys. J.* **2003**, *85*, 3035–3047.

(38) Richter, R. P.; Maury, N.; Brisson, A. R. *Langmuir* **2005**, *21*, 299–304.

(39) Reviakine, I.; Brisson, A. *Langmuir* **2000**, *16*, 1806–1815.

(40) Lussi, J. W.; Michel, R.; Reviakine, I.; Falconnet, D.; Goessl, A.; Csúcs, G.; Hubbell, J. A.; Textor, M. *Prog. Surf. Sci.* **2004**, *76*, 55–69.

(41) Michel, R.; Reviakine, I.; Sutherland, D.; Fokas, C.; Csúcs, G.; Danuser, G.; Spencer, N. D.; Textor, M. *Langmuir* **2002**, *18*, 8580–8586.

(42) Rossetti, F. F.; Reviakine, I.; Csúcs, G.; Assi, F.; Vörös, J.; Textor, M. *Biophys. J.* **2004**, *87*, 1711–1721.

(43) MacDonald, R. C.; MacDonald, R. I.; Menco, B. P. M.; Takeshita, K.; Subbarao, N. K.; Hu, L.-R. *Biochim. Biophys. Acta* **1991**, *1061*, 297–303.

(44) Rodahl, M.; Höök, F.; Krozer, A.; Brzezinski, P.; Kasemo, B. *Rev. Sci. Instrum.* **1995**, *66*, 3924–3930.

0.5 mL of temperature-equilibrated buffer. Measurements were performed on the third, fifth, and seventh overtones. For clarity, only the results obtained on the third overtone are reported, scaled by the overtone order.

Fluorescence Microscopy (FM). Fluorescence microscopy experiments were performed with a Zeiss LSM 510 Confocal Laser Scanning microscope (Carl Zeiss, Oberkochen, Germany) equipped with both a 25 mW Argon laser and a 1 mW HeNe laser, using either NBD-PC or TRITC-PE as the fluorescent species.

SPBs were prepared by incubating the substrates (clean TiO₂-coated glass slides or SiO₂/TiO₂ patterned surfaces) with vesicles suspended in the appropriate buffer. Excess vesicles were removed by rinsing with pure buffer. Observation typically began with bleaching a spot on the surface at full laser power. Recovery of fluorescence was taken to be indicative of bilayer formation,⁵ while no recovery indicated the presence of a vesicular layer. In the case of bilayer formation, diffusion coefficients were determined from the recovery curves according to Berquand et al.⁴⁵ (based on the theory published by Axelrod et al.⁴⁶ and Soumpasis⁴⁷).

Results

Supported Bilayers Are Formed on TiO₂ from Vesicles Containing More than 20% DOPS in the Presence of 2 mM Ca²⁺. The quartz crystal microbalance with dissipation (QCM-D) has become an established tool for studying the dynamics of biological interfaces.^{8,14,27,28,33,37,38,42,48–58} Numerous QCM-D studies of supported bilayer formation and vesicle adsorption on various surfaces^{27,28,33,37,38,51,55–58} allow an unambiguous interpretation of the QCM-D curves, such as those obtained when 100 nm vesicles containing various amounts of DOPS (a negatively charged phospholipid) were allowed to interact with TiO₂ in the presence of Ca²⁺ ions, that are known to bind to DOPS^{59–65} (Figure 2a). Between 0% and 10% of DOPS, these curves show an initial steady decrease (increase) in the frequency (dissipation factor) shift due to adsorption, followed by saturation at an asymptotic value. This result is consistent with previous findings.^{27,28} Vesicles containing more negatively charged DOPS in their

membranes elicited smaller asymptotic frequency and dissipation factor shifts (Figure 2a). In striking contrast to that, fluorescence intensity remained largely independent of DOPS content in the vesicles under these conditions (150 ± 8 and 147 ± 14 au for DOPC:DOPS 90:10 and DOPC vesicles, respectively; Figure 2b).⁶⁶ Therefore, in the presence of Ca²⁺, the number of vesicles on the surface remained approximately constant, regardless of DOPS content, for the compositions studied.

At 20% DOPS, extrema characteristic of supported bilayer formation appear in the QCM-D curves³³ (Figure 2a). SPB formation proceeded via a fusion or a fusion/decomposition pathway and required a critical surface density of the vesicles to commence.^{33,36,39}

Formation of supported bilayers under the above conditions was confirmed by fluorescence microscopy (Figure 2c). An SPB was distinguished from a layer of adsorbed vesicles (supported vesicular layer, or SVL³²) by bleaching a spot in the imaged area and recording the intensity inside the bleached spot as a function of time. In the case of an SVL, no recovery was observed (Figure 2b), while in the case of an SPB, the fluorescence intensity in the bleached area was found to recover to the initial value (Figure 2c). A diffusion coefficient of (2.2 ± 0.8) × 10⁻⁸ cm²/s (*n* = 7) for the NBD-PC probe in DOPC:DOPS 80:20 bilayers was calculated from the recovery data. This is consistent with the values reported in the literature for similar systems on other substrates.^{4,29} An SPB could also be formed in the presence of Ca²⁺ from a mixture containing 80% DOPC, 10% DOPS, and 10% biotin-X-DOPE (coupling of biotin renders this lipid negatively charged).

Influence of DOPS Content on Vesicle Adsorption to TiO₂ in the Absence of Ca²⁺. To better understand the details of vesicle–TiO₂ interactions, the effect of DOPS content on vesicle adsorption was studied in the absence of Ca²⁺. Bilayer formation was not observed in the absence of Ca²⁺ for any of the vesicle sizes and compositions investigated. The asymptotic frequency and dissipation factor shifts measured by QCM-D were found to decrease exponentially from the value observed in the absence of DOPS (that corresponds to a densely packed layer of vesicles) as a function of increasing DOPS content in the vesicles for all sizes studied (Figure 3a), reaching negligible values by ~20% DOPS⁶⁷ (a similar result has recently been reported for SiO₂ substrates, where cessation of adsorption was observed at a somewhat higher content of DOPS in the vesicles³⁷ (note that the two studies were done at different ionic strengths)). These results correlated well with those of fluorescence microscopy experiments, for which an exponential decrease in the fluorescence intensity as a function of DOPS content was also observed (Figure 3). This is clearly different from the observations in the presence of Ca²⁺ presented above, where fluorescence intensity was found to remain constant for those compositions that gave rise to intact vesicle adsorption. The decrease in the fluorescence intensity observed in the absence of Ca²⁺ points to a decrease in the number of vesicles adsorbed to the surface as a function of DOPS content in the membrane.

(45) Berquand, A.; Mazeran, P.-E.; Pantigny, J.; Proux-Delrouyre, V.; Laval, J.-M.; Bourdillon, C. *Langmuir* **2003**, *19*, 1700–1707.

(46) Axelrod, D.; Koppel, D. E.; Schlessinger, J.; Elson, E.; Webb, W. *Biophys. J.* **1976**, *16*, 1055–1069.

(47) Soumpasis, D. M. *Biophys. J.* **1983**, *41*, 95–97.

(48) Höök, F.; Rodahl, M.; Brzezinski, P.; Kasemo, B. *Langmuir* **1998**, *14*, 729–734.

(49) Höök, F.; Rodahl, M.; Brzezinski, P.; Kasemo, B. *J. Colloid Interface Sci.* **1998**, *208*, 63–67.

(50) Dultsev, F. N.; Ostanin, V. P.; Klenerman, D. *Langmuir* **2000**, *16*, 5036–5040.

(51) Pignataro, B.; Steinem, C.; Galla, H.-J.; Fuchs, H.; Janshoff, A. *Biophys. J.* **2000**, *78*, 487–498.

(52) Höök, F.; Kasemo, B.; Nylander, T.; Fant, C.; Sott, K.; Elwing, H. *Anal. Chem.* **2001**, *73*, 5796–5804.

(53) Glasmästar, K.; Larsson, C.; Höök, F.; Kasemo, B. *J. Colloid Interface Sci.* **2002**, *246*, 40–47.

(54) Otzen, D. E.; Oliveberg, M.; Höök, F. *Colloids Surf., B* **2003**, *29*, 67–73.

(55) Ekeröth, J.; Konradsson, P.; Höök, F. *Langmuir* **2002**, *18*, 7923–7929.

(56) Seantier, B.; Breffa, C.; Félix, O.; Decher, G. *Nano Lett.* **2004**, *4*, 5–10.

(57) Richter, R. P.; Brisson, A. *Langmuir* **2004**, *20*, 4609–4613.

(58) Weng, K. C.; Stalgren, J. J. R.; Duval, D. J.; Risbud, S. H.; Frank, C. W. *Langmuir* **2004**, *20*, 7232–7239.

(59) Harris, W. E. *Chem. Phys. Lipids* **1977**, *19*, 243–254.

(60) Choi, S. H.; Ware, W.; Lauterbach, S. R.; Phillips, W. M. *Biochemistry* **1991**, *30*, 8563–8568.

(61) Mattai, J.; Hauser, H.; Demel, R. A.; Shipley, G. G. *Biochemistry* **1989**, *28*, 2322–2330.

(62) Feigenson, G. W. *Biochemistry* **1989**, *28*, 1270–1278.

(63) Casal, H. L.; Martin, A.; Mantsch, H. H.; Paltauf, F.; Hauser, H. *Biochemistry* **1987**, *26*, 7395–7401.

(64) Feigenson, G. W. *Biochemistry* **1986**, *25*, 5819–5825.

(65) Gregory, D. P.; Ginsberg, L. *Biochim. Biophys. Acta* **1984**, *769*, 238–244.

(66) These values cannot be compared directly with those in Figure 3a, because the two sets were recorded with different settings of the microscope. On the other hand, care was taken to ensure that the microscope settings were identical within each set of experiments (the one reported here and the one reported in Figure 3).

(67) At these compositions, the preferential adsorption of vesicles on surface defects or along scratches significantly influences the measured frequency and dissipation shifts and may lead to larger values than expected.

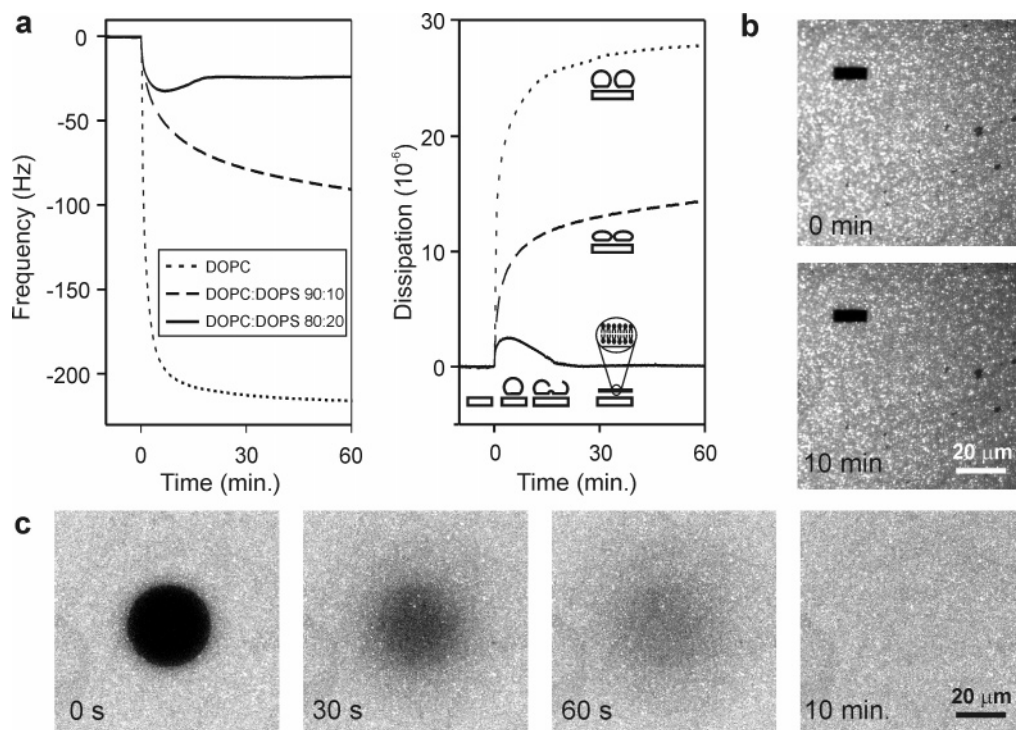


Figure 2. Influence of the DOPS content on the interactions of lipidic vesicles with TiO_2 in the presence of Ca^{2+} ions. (a) Adsorption of intact vesicles versus supported bilayer formation on TiO_2 followed by QCM-D (changes in the frequency are shown on the left, changes in the dissipation on the right; adsorption of material causes a decrease in the frequency. Dissipation factors are related to how flexible the layer is). When vesicles are deposited on the bare TiO_2 surface, they either stay intact, forming a supported vesicular layer at less than 20% DOPS (large asymptotic frequency and dissipation shifts, dotted and dashed lines), or open up to form a bilayer at 20% or more DOPS (extrema in frequency and dissipation indicating that the bilayer formation is preceded by vesicle adsorption and decomposition,³³ solid line). The stages corresponding to each part of the curves are sketched on the right plot. Lipid concentrations of 0.5 mg/mL (DOPC, DOPC:DOPS 9:1) and 0.05 mg/mL (DOPC:DOPS 8:2; this concentration was chosen to slow the bilayer formation down in order to obtain a clear bilayer formation curve) were used. In the cases where SPBs were formed, the total frequency shift was found to be $(26.0 \pm 1.3) \times n$ Hz, which corresponds to that reported in the literature for SPBs formed on SiO_2 .³³ (b) Fluorescence microscopy images of a supported vesicular layer formed on TiO_2 from vesicles containing 10 wt-% DOPS (dashed line in panel a). No sign of recovery of the intensity in the bleached spot is observed after 10 min, indicating that the species adsorbed on the surface are not laterally mobile. (c) Fluorescence microscopy images of a supported phospholipid bilayer formed on TiO_2 by adding vesicles containing 20 wt-% DOPS (solid line in panel a). The spot bleached in the center of the image recovers within 10–15 min, indicating the presence of a bilayer. The rather grainy appearance of the image might be due both to trapped intact vesicles and excess lipid material that did not arrange itself in a bilayer due to the fast kinetics of bilayer formation at this lipid concentration (0.5 mg/mL). We note that the bilayers formed on TiO_2 appear grainier than those formed on SiO_2 , but the reason for this is not clear.

Patterns of Supported Phospholipid Bilayers.

Richter et al.³⁷ have extensively characterized the interactions between DOPC:DOPS vesicles and silica. It is instructive to compare their results with those presented above for the titania surface: bilayer formation on silica occurs over a much broader range of conditions and does not always require Ca^{2+} . On TiO_2 , SPB formation from DOPS-containing vesicles always requires Ca^{2+} . Moreover, in the absence of Ca^{2+} , liposomes containing 20% DOPS or more do not adsorb to the surface. The exact origin of this behavior is discussed below (see Discussion). Here, it is described how these differences can be exploited for preparing patterns of bilayers on surfaces exhibiting a $\text{SiO}_2/\text{TiO}_2$ material contrast. The preparation of such surfaces with pattern sizes down to 200 nm has been reported previously.^{40,41}

The procedure, outlined in Figure 4, involves preparation of a bilayer on SiO_2 regions of the surface in the absence of Ca^{2+} from vesicles containing more than 20% DOPS, which do not adsorb to the titania regions (Figure 4a). This is followed by the preparation of another bilayer on titania in the presence of Ca^{2+} (Figure 4b). Vesicles used for bilayer preparation in both steps can contain guest molecules, thus imparting the desired, different functionalities on the silica and titania areas of the surface.

In the simplest case, shown in Figure 4c, two lipids bearing different fluorescent groups were incorporated into the two kinds of vesicles used in the bilayer formation steps. A bilayer containing NBD-PC (green) was formed on the silica surrounding $48 \times 48 \mu\text{m}^2$ TiO_2 squares, while a TRITC-PE-containing bilayer (red) was formed within the squares (the opposite distribution of labels has also been successfully achieved, not shown). Fluorescence recovery after photobleaching measurements confirmed that lipids in the bilayers formed on both surfaces were mobile. In most cases, a rim of vesicles appeared to be present between the TiO_2 and SiO_2 surfaces that did not recover when bleached. This could be due to complex surface chemistry and topography at the $\text{SiO}_2/\text{TiO}_2$ interface.

The patterns shown in Figure 4c were stable for at least 24 h with respect to intermixing of the two kinds of bilayers. This stability is likely due to the presence of a step between the two metal oxides⁴⁰ (Figure 4a,b) that acts as a diffusion barrier. This raises an intriguing question concerning the smallest height of such a step that is required to prevent intermixing. Adsorbed vesicles at the rim of the patterns could provide an additional diffusion barrier. (Others have used surface scratches or stripes of materials that do not support bilayer formation (such as alumina, titania, or partially oxidized poly-

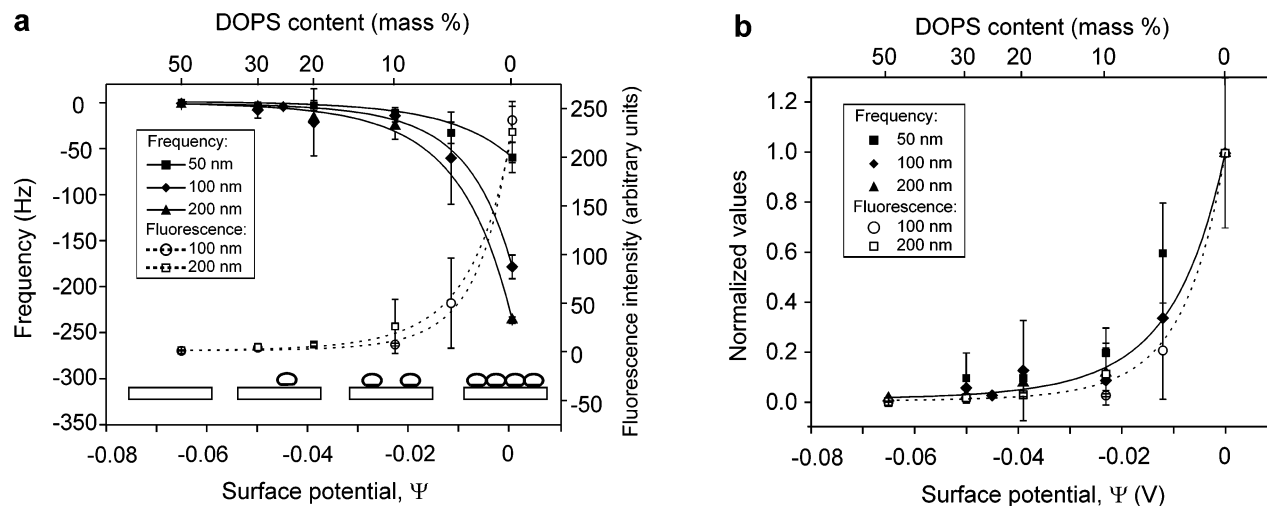


Figure 3. Influence of the DOPS content on the interactions of lipidic vesicles with TiO₂ in the absence of Ca²⁺ ions. For all compositions, vesicles were found to adsorb intact and form supported vesicular layers. (a) Fluorescence intensities and asymptotic frequency shifts from QCM-D are plotted as a function of surface potential of the vesicles for different vesicle sizes. The DOPS content is shown on the top axis. (See Supporting Information Figure 1 for the relationship between surface potential and DOPS content.) DOPC vesicles cover the surface completely at the concentrations used.²⁸ (b) In this plot, the data shown in (a) were normalized by the frequency shift (for QCM-D data) and the fluorescence intensity (for fluorescence data) in the absence of DOPS. The normalized plots are well-described by a curve of the form $e^{A(\Psi^2 - B\Psi)}$, where Ψ is the surface potential of the vesicles, $A = 4 \cdot E^2 \cdot n \cdot \delta \cdot S / (k \cdot T)^2 \cdot \kappa \cdot \Delta$, $B = \Psi_s / \delta$, $\Delta = e^{\kappa l} - e^{-\kappa l}$, $\delta = e^{-\kappa l} / 2$, $\kappa = \sqrt{2 \cdot n \cdot E^2 / \epsilon \cdot \epsilon_0 \cdot k \cdot T}$ is the inverse Debye length, Ψ_s is the surface potential of TiO₂, l is the distance between the oxide surface and the maximum of the energy barrier, k is Boltzman's constant, T is the temperature, n is the concentration of the electrolyte in m⁻³, E is the elementary charge, and ϵ_0 and ϵ are the dielectric permeability of vacuum and water, respectively. S is a fitting parameter, which has the units of area (m²). This expression was obtained from eq 38 in Parsegian and Gingell⁷⁹ in the following manner: the normalized response, y_i/y_0 , where y_i is the response at a given DOPS content and y_0 is the response in the absence of DOPS, is given by $e^{-(\Delta G_i/kT) - (\Delta G_0/kT)}$, where ΔG_0 and ΔG_i are the free energies of interaction between the negatively charged TiO₂ surface and DOPS-free or DOPS-containing vesicles, respectively. These, in turn, are given by eq 38 in Parsegian and Gingell.⁷⁹ A satisfactory fit to the data was obtained by varying the value of S while keeping $l \approx 0.8$ nm and $\Psi_s = -40$ mV constant (these values were found to give the best fits). S varied slightly with the vesicle size, but this variation was not significant given the experimental errors. For QCM data, values in the range of 12.1–13.2 nm² were obtained (the solid line in the plot corresponds to a fit with $S = 12.8$ nm²), while for fluorescence data, 16.2–16.8 nm² (dotted line, $S = 16.4$ nm²). This difference is most likely due to the fact that, as we have recently shown, the acoustic response is not a linear function of vesicle surface concentration,²⁸ and the normalized response will contain other terms (although the fact that the data could be fit at all to the above expression suggests that these terms do not modify the functional form of the dependence). Further quantitative evaluation of the barrier height is impossible, however, because Parsegian's expressions are only applicable to the cases where Ψ is small or κl is large, neither of which is true in our case.

(dimethylsiloxane)) to form diffusion barriers and separate bilayers by nonbilayer regions^{15,16,68–70}.)

To test the ability of the SPB corrals (term coined by Groves et al.⁶⁸), such as those shown in Figure 4c, to serve as a platform for the design of "smart", bio-interactive interface based on TiO₂ (similar interfaces based on bilayer patterns formed on a SiO₂/Au template have been reported²¹), two types of functional lipids, biotinylated lipids and Ni-chelator lipids,⁷¹ were incorporated into the vesicles used in the SPB formation steps. This resulted in the formation of a biotinylated bilayer on silica and Ni-bearing bilayer on TiO₂. The former was loaded with streptavidin and fluorescently labeled biotinylated vesicles, while the latter was loaded with histidine-tagged green fluorescent protein (Figure 4d,e). Some degree of nonspecific interactions of the protein with the bilayers not carrying Ni-NTA was observed, despite the recognized protein-resistant properties of supported bilayers.⁵³ The use of negatively charged (DOPS-exposing) bilayers may also have a thrombogenic effect in the body due to the initiation of a blood clotting cascade.⁷² Both of these issues might be

resolved by adding cationic molecules to the formed bilayer that will sequester the DOPS lipids.

Discussion

Interpretation of the Acoustic Response from Surface-Adsorbed Vesicles. Both in the presence and in the absence of Ca²⁺, the acoustic response (frequency and dissipation shifts) decreases as a function of DOPS content in the vesicles. However, in the presence of Ca²⁺, the fluorescence intensity does not depend on DOPS content, suggesting that the number of vesicles on the surface does not change as a function of DOPS. In the absence of Ca²⁺, on the other hand, there is a decrease in the number of vesicles adsorbed on the surface. Therefore, the causes for the decrease in the acoustic response are quite different in the two cases.

In principle, there can be two reasons for a decrease in the acoustic response from SVLs: a decrease in the number of vesicles adsorbed on the surface or a decrease in the height of the adsorbed vesicles.⁷³ We therefore conclude that, while in the absence of Ca²⁺, the decrease in the acoustic response as a function of DOPS content is due to the diminishing number of vesicle adsorbed on the surface, in its presence, it is due to the diminishing thickness of the SVLs, the number of vesicles within which remains

(68) Groves, J. T.; Ulman, N.; Boxer, S. G. *Science* **1997**, *275*, 651–653.

(69) Cremer, P. S.; Groves, J. T.; Kung, L. A.; Boxer, S. G. *Langmuir* **1999**, *15*, 3893–3896.

(70) van Oudenaarden, A.; Boxer, S. G. *Science* **1999**, *285*, 1046–1048.

(71) Schmitt, L.; Dietrich, C.; Tampé, R. *J. Am. Chem. Soc.* **1994**, *116*, 8485–8491.

(72) Zwaal, R. F. A.; Comfurius, P.; Bevers, E. M. *Biochim. Biophys. Acta* **1998**, *1376*, 433–453.

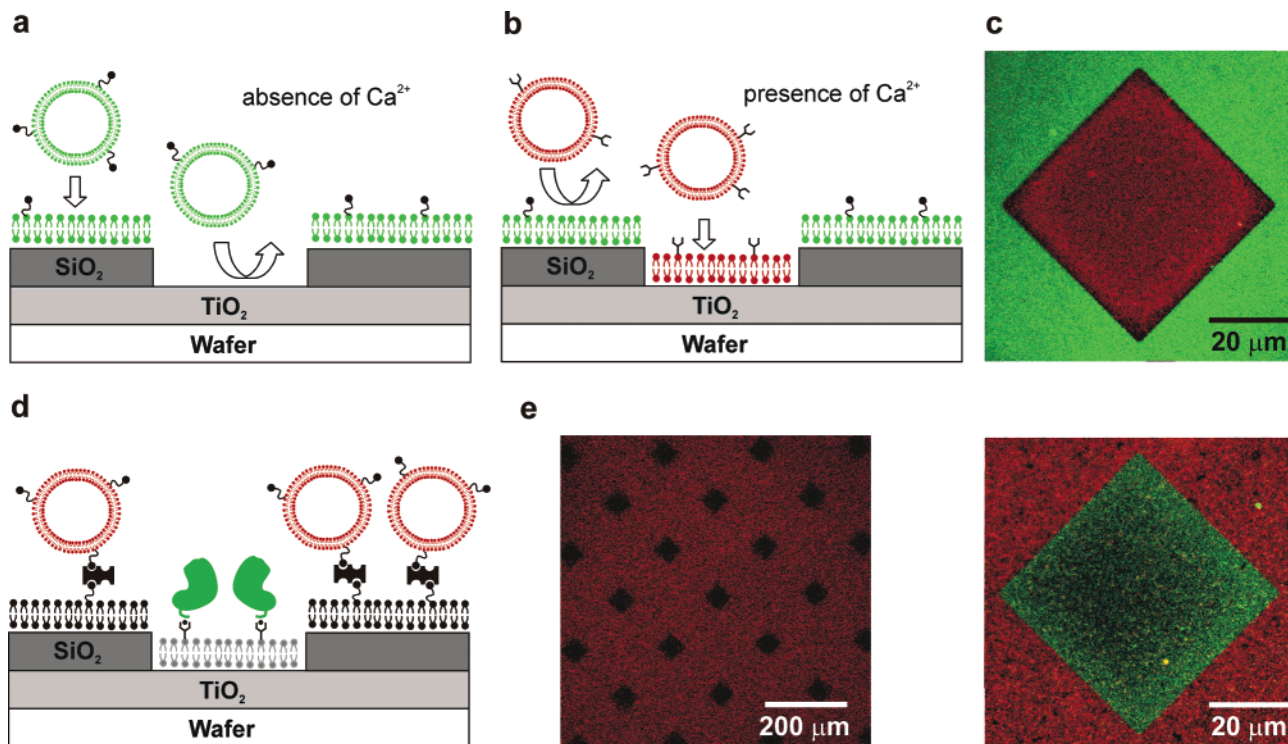


Figure 4. Using the selectivity of lipidic vesicles to prepare patterns of SPBs. (a) Vesicles containing between 50% and 20% DOPS are added in the absence of Ca^{2+} to a substrate that exhibits a $\text{SiO}_2/\text{TiO}_2$ contrast. A bilayer is formed on SiO_2 , while the electrostatic repulsion does not allow the vesicles to adsorb on TiO_2 . (b) The second type of vesicles, containing more than 20% DOPS, is added to the substrate in the presence of Ca^{2+} . A second kind of bilayer is formed on the TiO_2 regions of the sample. The presence of the first bilayer on the SiO_2 regions prevents vesicle adsorption on those regions. (c) Fluorescence microscopy image of a TRITC-labeled DOPC:DOPS 80:20 bilayer formed in Ca^{2+} buffer on TiO_2 (red) surrounded by a NBD-labeled DOPC:DOPS 80:20 bilayer formed in EDTA buffer on SiO_2 (green). The image was taken 10 h after formation of the bilayers and shows no sign of intermixing of the two kinds of bilayers. (d) Lipids carrying various functionalities (biotin, the Ni-chelator NTA, etc.) can be incorporated in the SPB patterns, thus allowing for the specific immobilization of different molecules (i.e., biotinylated vesicles or his-tagged proteins) on each side of the pattern. (e) Fluorescence microscopy images corresponding to the situation depicted in panel d. Left: overview image of biotinylated DOPC vesicles (red) immobilized via streptavidin on a biotinylated SPB. Right: his-tagged green fluorescent protein (green) immobilized on an SPB containing Ni-NTA lipids, surrounded by biotinylated DOPC vesicles (red) immobilized via streptavidin on a biotinylated SPB.

approximately constant. In other words, the height of the adsorbed vesicles decreases as the content of DOPS within them increases.

In the Presence of Ca^{2+} , Liposomes Containing More DOPS Adhere Stronger to TiO_2 . The extent of deformation of a vesicle in contact with a surface is determined by the effective adhesion strength. The latter is given by $w \equiv WR^2/\kappa_b$, where W is the value of the vesicle–surface interaction potential at its minimum (Figure 5), κ_b is the bending modulus of the bilayer, and R is the vesicle radius; that is, vesicle adhesion is a result of a competition between vesicle–surface attraction and bilayer rigidity (which opposes bending).⁷⁴ Therefore, a larger extent of deformation (smaller height) implies a stronger adhesion (larger values of w), which can either be the result of an increase in the lipid– TiO_2 attraction (characterized by W), or a decrease in the bending modulus of the bilayer, as a function of DOPS.^{74–76} The former scenario is schematically depicted in Figure 5. When the strength of adhesion becomes sufficiently strong (e.g., in

the case of vesicles containing at least 20% DOPS), a bilayer is formed.

In the Absence of Ca^{2+} , There Is an Energy Barrier of Electrostatic Origin That Prevents Vesicles from Reaching the Surface. We have shown above that when Ca^{2+} is absent, fewer and fewer vesicles adsorb to TiO_2 as the DOPS content of the vesicles increases. A decrease in the number of surface-bound vesicles can be caused by an energy barrier that prevents vesicles from coming into contact with the surface. The height of such a barrier should be a function of the vesicle surface potential (given by DOPS content and ionic strength^{77,78}). The situation is schematically depicted in Figure 5. Indeed, QCM-D and fluorescence data acquired in the absence of Ca^{2+} and normalized by the response in the absence of DOPS collapsed onto similar curves for the response (fluorescence intensity, frequency, or dissipation) versus surface potential of the vesicles (the slight difference of the normalized response curves obtained from QCM-D data and fluorescence data is attributed to the nonlinearity of the

(73) The dominant contribution to the frequency shift observed by QCM-D is proportional to the mass per unit area of the adsorbed layer. Mass per unit area of a layer is, in turn, the product of layer density and thickness. The former remains approximately constant (close to the density of water). Therefore, the differences in the acoustic responses between two layers with similar numbers of vesicles adsorbed are due to the differences in the thicknesses of the two layers.

(74) Seifert, U.; Lipowsky, R. *Phys. Rev. A* **1990**, *42*, 4768–4771.

(75) Seifert, U. *Adv. Phys.* **1997**, *46*, 13–137.

(76) According to dynamic light scattering measurements, vesicle size remains nearly constant as a function of DOPS (not shown; the effect vesicle radius has on the frequency shift in the case of surface-adsorbed vesicles is discussed in detail in Reimhult et al.⁸⁸ and Reviakine et al.²⁶).

(77) Eisenberg, M.; Gresalfi, T.; Riccio, T.; McLaughlin, S. *Biochemistry* **1979**, *18*, 5213–5223.

(78) Ohki, S.; Düzgünes, N.; Leonards, K. *Biochemistry* **1982**, *21*, 2127–2133.

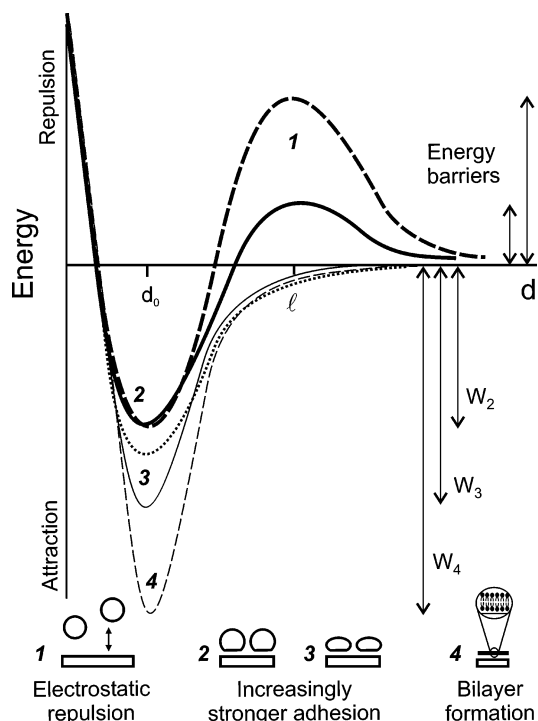


Figure 5. Summary of the interactions between TiO₂ and vesicles of different compositions. A diagram showing what the interaction energy between DOPC:DOPS vesicles and the TiO₂ surface may look like under various conditions. Numbers next to the curves refer to cartoons depicting the relevant situation (shown at the bottom of the figure). Thick lines: the situation in the absence of Ca²⁺ for vesicles with low (solid line) and high (dashed line) content of DOPS; vesicles need to overcome an energy barrier to reach the surface. The height of the barrier is a function of DOPS content, and its location is given by the value of l (see also Figure 3). If the barrier is sufficiently high (as is the case for >20% DOPS), no adsorption occurs (cartoon 1). There remains a short-range attractive component to the vesicle–surface interactions, however, which prevents the vesicles that do adsorb (e.g., vesicles containing less DOPS) from desorbing (cartoon 2). We attribute this attractive interaction to that between TiO₂ and DOPC (dotted curve; no distinction is made between the situations in the presence and in the absence of Ca²⁺ for reasons of clarity), and therefore the minima in these three curves are drawn to be of similar depth (W refers to the value of the vesicle–surface interaction potential at the minimum⁷⁹). It is currently not possible to ascertain how this short-range attraction depends on DOPS contents. Whether an energy barrier exists also in the case of DOPC–TiO₂ interactions is also not known at present, but in any case it is of the order kT . In the presence of Ca²⁺ (curves and cartoons 3 and 4), the energy barrier is lowered or abolished. Furthermore, there is an increase in the adhesion strength between the vesicles and the surface as a function of DOPS content in the vesicles. As discussed in the text, this could be due to the increase in the strength of the attractive interactions between vesicles and the surface, characterized by W (this is the case depicted in this diagram, in which the minimum gets deeper from 3 to 4). It is also possible that the increase in the adhesion strength is caused by a decrease in the bending modulus of the vesicles or by a combination of the two factors (not shown). In either case, it results in the corresponding increase in the vesicle deformation (cf., cartoons 2 and 3) and finally leads to bilayer formation (cartoon 4).

acoustic response of the QCM-D as a function of vesicle surface concentration,²⁸ Figure 3b) that was well-described by an exponential of the form $y = e^{A(\Psi^2 - B\Psi)}$, where Ψ is the surface potential of the vesicles and A and B are defined in the legend of Figure 3 (cf., eq 38 in Parsegian and Gingell⁷⁹). The absolute value of the term $A(\Psi^2 - B\Psi)$ gives the height of the energy barrier (Figure 3, Figure 5).

Theoretical analysis of surface-adsorbed vesicles⁷⁵ predicts the existence of a critical adsorption radius, R_a , below which vesicles do not adsorb. However, in the presence of an energy barrier, vesicles with $R > R_a$ may be prevented from reaching the surface in a first place. Under such circumstances, R_a will not be observed.

It is interesting to note that the adhesion of vesicles to the surface remains sufficiently strong for the vesicles that do adsorb to withstand rinsing with the vesicle-free buffer (e.g., in the case of vesicles containing 5% and 10% DOPS, Figure 3). This implies that the barrier to desorption is higher than the barrier to adsorption. In other words, there remains a short-range attractive component to the interaction between the DOPS-containing vesicles and the surface. Most probably, this component is due to DOPC.

Interactions between TiO₂ and DOPS-Containing Liposomes: Role of Ca²⁺. Based on the above discussion, one clear role of Ca²⁺ is to reduce or abolish the energy barrier that arises due to electrostatic repulsion between the negatively charged oxide and vesicle surfaces. This allows a sufficient number of vesicles to adsorb to the oxide surface to form the densely packed SVLs that are required for SPB formation to proceed by the fusion or fusion/decomposition pathway.^{33,36,39}

However, a mere presence of a densely packed SVL on the surface of TiO₂ is not sufficient to lead to SPB formation.^{27,28,32,33,39} An adequate adhesion strength of the vesicles to the surface is required as well, and in fact we have shown that in the presence of Ca²⁺, the effective adhesion strength (w) increases with DOPS content. This occurs despite the fact that, even after Ca²⁺ is bound to the vesicles, both their surface charge density and the absolute value of their (negative) surface potential also increase^{77,78} (Supporting Information Figure 1). We therefore conclude that the second role of Ca²⁺ is to mediate a short-range attraction between the vesicles and the TiO₂ surface, stronger than that observed between DOPC and TiO₂.

A pertinent question is whether Ca²⁺ accomplishes both of these tasks by binding to the vesicles only, or whether it also binds to the oxide surface. While at present we cannot distinguish between these two situations clearly, several lines of evidence lead us to conjecture that Ca²⁺ binds to both the vesicles and the oxide surfaces.⁸⁰ First, interactions of pure DOPC vesicles with the substrate were found to depend on whether Ca²⁺ is present or not, despite the fact that only ~0.1% of DOPC molecules are expected to be occupied by Ca²⁺ ions under our experimental conditions.^{81,82} This can be deduced from the QCM-D data, which show that DOPC vesicles adsorbed in the presence of Ca²⁺ give rise to a larger frequency shift than vesicles adsorbed in its absence (~240 ± 27 Hz as compared to 177 ± 17 Hz; cf., the behavior of 100 nm DOPC vesicles in Figure 2 and Figure 3). Given that a fully packed SVL is already formed in the absence of Ca²⁺,²⁸ this indicates that a thicker layer is formed in the presence of Ca²⁺ than in its absence. Thus, the adhesion strength of DOPC vesicles to TiO₂ is weakened by Ca²⁺. A further

(79) Parsegian, V. A.; Gingell, D. *Biophys. J.* **1972**, *12*, 1192–1204.

(80) We have measured the ξ -potential of ~200 nm TiO₂ particles in the presence and in the absence of 2 mM Ca²⁺, and found that in its presence, the ξ -potential was dramatically reduced (from -33 ± 1 to -3 ± 1 mV). Our measurements of IEP and of the zeta-potential in the absence of Ca²⁺ are consistent with published values.⁸⁹ Ongoing experiments will help elucidate the affinity of Ca²⁺ for the oxide surface.

(81) McLaughlin, A.; Grathwohl, C.; McLaughlin, S. *Biochim. Biophys. Acta* **1978**, *513*, 338–357.

(82) Lis, L. J.; Lis, W. T.; Parsegian, V. A.; Rand, R. P. *Biochemistry* **1981**, *20*, 1771–1777.

support for this argument comes from the fact that the frequency shift observed at 10% DOPS in the presence of Ca^{2+} was similar to that observed at 0% DOPS in its absence, for the same vesicle size and concentration (not shown), suggesting that vesicles in these two experimental conditions are deformed to a similar extent.

Second, others have arrived at a conclusion that Ca^{2+} binds to titanium oxide,⁸³ and, finally, Ca^{2+} has previously been shown to significantly affect the process of SPB formation from EggPC vesicles on mica,³⁹ to which it is known to bind.^{84,85} Similarly, Mg^{2+} was found to have a comparable effect on the behavior of EggPC vesicles on $-\text{OPO}_3$ and $-\text{OSO}_3$ modified gold surfaces, to which it also binds⁵⁵.

The influence surface-bound ions have on vesicle adsorption and bilayer formation evident from previous studies^{39,55} and conjectured here points to a strong possibility that the differences in the ability of different surfaces to bind ions significantly contribute to the observed differences in vesicle–surface interactions. This issue has not yet been investigated to any significant degree, and further experiments are clearly in order.

Ca^{2+} -mediated short-range attraction between the two surfaces may result from the latter bridging the charged groups on TiO_2 and those on the vesicles (cf., Ellingsen⁸³), in the same manner it bridges PS molecules in the opposing lipid bilayers.^{59,60,62,64} A more general effect of Ca^{2+} binding may also be responsible: Chavez et al.⁸⁶ have concluded that the attraction between a dipolar surfactant and a surface was strongest near the isoelectric point of the surface, that is, when most of the surface charges were neutralized by counterions and replaced by surface dipoles.

Concluding Remarks

In summary, we have shown how to prepare supported bilayers of various compositions from DOPS-containing liposomes on TiO_2 surfaces in the presence of Ca^{2+} . A short-range TiO_2 –DOPS interaction mediated by Ca^{2+} is proposed to provide the driving force for the bilayer formation.

In the absence of Ca^{2+} , bilayer formation was not observed, and adsorption of vesicles was prevented by an energy barrier of electrostatic origin.

Supported bilayer corrals that incorporated various functionalities were prepared on $\text{TiO}_2/\text{SiO}_2$ patterned substrates. This patterning method relies on the unique ability of lipidic vesicles to distinguish between different surfaces. The system described provides substantial versatility with respect to the functionalities that can be incorporated into the SPB corrals. Biotinylated nucleic acids have previously been bound to streptavidin-bearing SPBs and are easy to incorporate into the protocol developed above.¹⁴ Gangliosides, that often serve as

receptors for pathogenic bacteria, can be incorporated into the bilayers, thus making possible the design of pathogen-sensing biosensors. Advances in synthetic organic chemistry have produced peptide-bearing lipids that can serve as receptors for cell attachment,⁸ and the Ni-chelator lipids/histidine tagged protein technology provides limitless possibilities for incorporating soluble proteins into the patterning strategy. Use of liposomes with asymmetric lipid distribution between the two leaflets⁸⁷ may be required to ensure that the bulky headgroups of the guest lipids do not interfere with the SPB formation process. More important perhaps is the possibility of integrating hydrophobic moieties, from lipophilic drugs to transmembrane proteins, into the SPBs. The ability to prepare such functional interfaces on the basis of a widely used biomaterial such as titanium constitutes a crucial advance in the research on interactive bio-interfaces.

These results enhance the general understanding of liposome–surface interactions and open a new chapter in the research on TiO_2 -based biointeractive interfaces.

Acknowledgment. We thank Drs. Janos Vörös (Swiss Federal Institute of Technology, Zürich), Fabiano Assi (Baverstam Associates, Geneva, Switzerland), Alexander N. Morozov (University of Leiden, Leiden, The Netherlands), Prof. Bengt Kasemo (Chalmers Institute of Technology, Gothenburg, Sweden), and Prof. Fredrik Höök (Lund University, Lund, Sweden) for insightful comments and stimulating discussions, Prof. Steven Boxer (Stanford) for pointing out to us that the result of Thompson et al. may be due to SiO_2 contamination of their TiO_2 surfaces, Dr. Mattias Rudh and Hans Green (Q-Sense AB, Gothenburg, Sweden) for superb support of the QCM-D instrument, Dr. Didier Falconnet for the production of the patterned substrates, Gouliang Zhen, M.Sc., and Dr. Eva Künemann for providing His-tagged GFP, Dr. Gabor Csucs (Swiss Federal Institute of Technology, Zürich) for assistance with the fluorescence microscopy measurements, and Prof. Edgar Stüssi (Swiss Federal Institute of Technology, Zürich) for allowing F.F.R. to use their fluorescent microscopy facilities. This project was funded by the Swiss Top Nano 21 program (KTI project # 5493-1 and 6348-1), EU Framework Program 6 (Project “NANOCUES”), and the European Science Foundation Program “Self-Organized Nanostructures” (SONS, Project “NanoSMAP”).

Supporting Information Available: Plot of the surface potential of vesicles as a function of DOPS content in the presence and in the absence of Ca^{2+} ions. This material is available free of charge via the Internet at <http://pubs.acs.org>.

LA0509100

(87) Pautot, S.; Frisken, B. J.; Weitz, D. A. *Proc. Natl. Acad. Sci. U.S.A.* **2003**, *100*, 10718–10721.

(88) Reimhult, E.; Höök, F.; Kasemo, B. *J. Chem. Phys.* **2002**, *117*, 7401–7404.

(89) Rezwani, K. Protein treated aqueous colloidal oxide particle suspensions: Driving forces for protein adsorption and conformational changes. Dissertation Nr. 15882, ETH Zürich, 2005.

(83) Ellingsen, J. E. *Biomaterials* **1991**, *12*, 593–596.

(84) Pashley, R. M.; Israelachvili, J. N. *J. Colloid Interface Sci.* **1984**, *97*, 446–455.

(85) Pashley, R. M. *J. Colloid Interface Sci.* **1981**, *83*, 531–546.

(86) Chavez, P.; Ducker, W.; Israelachvili, J.; Maxwell, K. *Langmuir* **1996**, *12*, 4111–4115.